Turkish Journal of Earth Sciences

Volume 32 | Number 2 Article 4

1-1-2023

The first application of the luminescence surface exposure dating method on active fault scarps in the Western Anatolia extensional province: the Manisa Fault as an example

MUSTAFA SOFTA

EREN ŞAHİNER

HASAN SÖZBİLİR

JOEL QG SPENCER

MEHMET UTKU

See next page for additional authors

Follow this and additional works at: https://journals.tubitak.gov.tr/earth

 Part of the Earth Sciences Commons

Recommended Citation

SOFTA, MUSTAFA; ŞAHİNER, EREN; SÖZBİLİR, HASAN; SPENCER, JOEL QG; UTKU, MEHMET; and BÜYÜKTOPCU, MEHMET FATİH (2023) "The first application of the luminescence surface exposure dating method on active fault scarps in the Western Anatolia extensional province: the Manisa Fault as an example," *Turkish Journal of Earth Sciences*: Vol. 32: No. 2, Article 4. https://doi.org/10.55730/1300-0985.1836

Available at: https://journals.tubitak.gov.tr/earth/vol32/iss2/4

This Article is brought to you for free and open access by TÜBİTAK Academic Journals. It has been accepted for inclusion in Turkish Journal of Earth Sciences by an authorized editor of TÜBİTAK Academic Journals. For more information, please contact academic.publications@tubitak.gov.tr.

The first application of the luminescence surface exposure dating method on active fault scarps in the Western Anatolia extensional province: the Manisa Fault as an example

Authors
MUSTAFA SOFTA, EREN ŞAHİNER, HASAN SÖZBİLİR, JOEL QG SPENCER, MEHMET UTKU, and MEHMET FATİH BÜYÜKTOPCU

This article is available in Turkish Journal of Earth Sciences: https://journals.tubitak.gov.tr/earth/vol32/iss2/4

TÜBİTAK

Turkish Journal of Earth Sciences

http://journals.tubitak.gov.tr/earth/

Research Article

Turkish J Earth Sci
(2023) 32: 163-180
© TÜBİTAK
doi:10.55730/1300-0985.1836

The first application of the luminescence surface exposure dating method on active fault scarps in the Western Anatolia extensional province: the Manisa Fault as an example

Mustafa SOFTA[1,3,*], Eren ŞAHİNER[2], Hasan SÖZBİLİR[1,3], Joel Q.G. SPENCER[4], Mehmet UTKU[5], M. Fatih BÜYÜKTOPÇU[3]

[1]Department of Geological Engineering, Dokuz Eylül University, İzmir, Turkey
[2]Luminescence Dating Research Laboratory, Earth Sciences Application and Research Center (YEBİM), Ankara University, Ankara, Turkey
[3]Earthquake Research and Implementation Center of Dokuz Eylül University, İzmir, Turkey
[4]Department of Geology, Kansas State University, Manhattan, USA
[5]Department of Geophysical Engineering, Dokuz Eylül University, İzmir, Turkey

Received: 20.09.2022 • **Accepted/Published Online:** 13.01.2023 • **Final Version:** 27.03.2023

Abstract: While there has been significant research on the dating of paleoearthquakes using methods such as surface cosmogenic dating, and trench-based luminescence or radiocarbon dating, this paper focuses on implementing an alternative surface dating method using a fault scarp-based optically stimulated luminescence (OSL) dating approach. Hence for the first time, we investigated the Pleistocene to Holocene earthquake cycle of the Manisa Fault, one of the dip-slip active faults of the Western Anatolia extensional province, utilizing novel OSL surface exposure techniques. In this technique, OSL bleaching profiles on the fault surface are directly related to the exposure of the fresh fault scarps that are produced by earthquakes. The results indicate that the Manisa Fault is responsible for at least six surface rupturing earthquakes since the Holocene, occurring at 154 ± 22 year (E6: LSD3), 416 ± 48 year (E5: LSD4), 1103 ± 82 year (E4: LSD5), 2067 ± 138 year (E3: LSD6), 5376 ± 48 year (E2: LSD7), and 6432 ± 218 year (E1: LSD8). Our results of the first use of this novel method on the Manisa Fault are in agreement with prior cosmogenic dating of fault scarps and trench-based paleoseismological chronological data, and we conclude that the OSL surface chronology is a promising alternative for fault scarp dating of paleoearthquakes.

Key words: OSL surface dating, earthquakes, Manisa Fault, paleoseismology

1. Introduction

Earthquake hazard is primarily estimated from historical earthquakes in paleoseismological studies (e.g., Wallace, 1981; McCalpin, 2009; Meghraoui and Atakan, 2014), instrumental seismicity in seismic studies (e.g., Campbell, 1982, 1983; Pisarenko et al., 1996; Akkar et al., 2018; Nas et al., 2020), and modern-day measurements of strain in geodetic studies (e.g., Bürgmann et al., 1997; Reilinger et al., 2006, 2010; Aktuğ et al., 2013, 2021). Of these, paleoseismology is a common multidisciplinary technique used to determine the quantitative cycle of historical earthquakes. Paleoseismology studies are carried out both on surface traces of active faults and on fault planes using trench-based and surface-based techniques, respectively. Also, one should note that core-based paleoseismology—known as subaqueous paleoseismology—is one of the most popular alternative paleoseismic techniques.

A detailed search of the literature on the "Web of Science" and "Google Scholar" websites between 1986 and 2022 reveals there are 1185 articles with keywords "Paleoseismology" OR "Palaeoseismology" (Softa and Utku, 2022). In many of these studies, recent earthquakes that occurred on a fault can be revealed in paleoseismic trenches where offset sedimentary layers can be dated by radiocarbon and/or luminescence techniques. Of these 1185, the number of articles focusing on luminescence dating and trench-based modeling is 88. Furthermore, there are eleven trench-based paleoseismology studies published using luminescence and radiocarbon dating methods in Western Anatolia (e.g., Pavlides et al., 2006; Kürçer et al., 2017; Özaksoy et al., 2018; Dikbaş et al., 2018; Kürçer et al., 2019, 2021; Basmenji et al., 2021; Duran et al., 2021; Civico et al., 2021; Dikbaş et al., 2022; Şengöçmen Geçkin et al., 2022).

Faulting on timescales larger than ten thousand years can be constrained by time-averaged fault slip rates, which are determined by dating fault-offset sedimentary deposits or rock bodies. Various Quaternary geochronological techniques can be used to establish the age of offset deposits/rocks, but each method has advantages and

* Correspondence: mustafa.softa@deu.edu.tr

This work is licensed under a Creative Commons Attribution 4.0 International License.

limitations, which are technique- dependent, and are determined by factors such as variation in bedrock geology, complications of age construction, or absence of organic material (e.g, Softa et al., 2021, 2022).

In recent years, luminescence dating has been applied to geological problems by constraining sedimentary depositional age from features such as glacial landforms, fan deposits, colluvial wedges, and terrace levels (e.g., Lee et al., 2001; Prentice et al., 2002; Owen et al., 2003; Spencer and Owen, 2004; Lukas et al., 2007; Preusser et al., 2008; Rittenour, 2008; Spencer and Robinson, 2008; Fattahi et al., 2010; Rhodes, 2011; Gurrola et al., 2014; Hu et al., 2015; Schildgen et al., 2016; Stahl et al., 2016; Tsodoulos et al., 2016; Trexler et al., 2020; Erturaç, 2021; Softa et al., 2021).

In addition to the well-established application of trapped-charge luminescence phenomena to the dating of a variety of sedimentary features as indicated above, methods have also been developed to use luminescence for dating rock surfaces (Liritzis, 2011; Sohbati et al., 2012a,b). The optically stimulated luminescence (OSL) surface dating technique is a novel application of trapped-charge luminescence with a dating range spanning late Quaternary timescales. The OSL surface dating approach yields similar chronological information to OSL dating of sedimentary deposits by measuring the last exposure to daylight for minerals collected from a rock surface (Lehman et al., 2018). Moreover, the method can be used to estimate the exposure time of a surface to daylight.

Since its development a number of articles have documented the increased utilization of the OSL surface dating method, but the technique has not been applied to dating of fault surfaces until May of 2022 (Softa et al., 2022). After this work, a prominent study of the successful application to fault surfaces was published by Luo et al. (2022). This method utilizes luminescence stimulated from quartz, feldspar, or other minerals present in most lithologies. The work of Softa et al. (2022), Luo et al. (2022) and the study presented here are pioneering research in the application of the OSL surface dating technique directly on the fault surface to quantify paleoseismic activity of active faults in Turkey and China.

Currently, fault surface-based studies mostly apply cosmogenic radionuclide (CRN) dating methods to determine the timing of historical earthquakes by measuring the concentration of rare cosmogenic nuclides in fault scarp (e.g., Zreda and Noller, 1998; Gosse and Philips, 2001; Mitchell et al., 2001; Benedetti et al., 2002, 2003; Palumbo et al., 2004; Ivy-Ochs and Kober, 2008; Dunai, 2010). In addition to that, the electron spin resonance technique on fault clays has been used to evaluate paleoseismological events in fault scarp (e.g., Lee and Schwarcz, 1994), and luminescence dating methods have been applied to liquefaction features (e.g., Banerjee etal., 1997; Porat et al., 2007; Thomas et al., 2007) and fault gouge (e.g., Singhvi et al., 1994; Ding and Lai, 1997; Banerjeeet al., 1999; Mukul et al., 2007; Spencer et al., 2012; Tsakalos et al., 2020).

Recently, paleoseismology of the Manisa Fault (MF) (western segment) was reconstructed using CRN scarp dating (Akçar et al., 2012; Mozafari et al., 2021). In addition to surface dating methods, trench based paleoseismology with radiocarbon and luminescence dating methods was applied to western (Özkaymak et al., 2011) and eastern segments (Duran et al., 2021) of the MF. However, the studies regarding surface-based paleoseismology of the eastern segment of MF aim to unravel the produced Pleistocene and Holocene earthquake activities has not been addressed. In addition to that, albeit the historical earthquake catalogs well reflect the damage dimension on the Aegean region, and the most popular tool for paleoseismological studies, the regarding on how the relied on the historical catalogs which were prepared eyewitness and uncertain location problems are continues. Therefore, in order to eliminate such problems/uncertainty and bridge the gap in the existing literature makes the essential point that an appropriate Quaternary dating method must be implemented on the faulted rock in paleoseismological studies.

In this study, we suggest an alternative surface dating method, and demonstrate its application to fault surfaces by measuring the Pleistocene to Holocene earthquake cycles of the normal fault system of the MF in Western Anatolia, utilizing novel OSL surface exposure techniques. The luminescence depth profile measured above and below the present-day surface on a bedrock fault scarp is directly related to the exhumation of the fault scarp and can elucidate fault behavior over multiple earthquake cycles. In short, the novel OSL surface chronology not only gives an alternative way of scarp dating but also supports the description of the paleoseismological history of this area.

2. Tectonic settings and seismicity

Western Anatolia is being actively deformed as a result of the continental collision between Africa, Arabia, and Eurasia (e.g., Şengör et al., 1985; Royden, 1993; Bozkurt, 2001) (Figure 1a). Modern-day measurements of strain based on GPS velocities indicate rates of extension of 20 mm/year, making Western Anatolia one of the fastest extending regions on Earth (Aktuğ et al., 2013). Highly seismically active, the eastern Mediterranean region has been extending obliquely since the Miocene (e.g., Bingöl, 1976; Le Pichon and Angelier, 1979; Barka and Reilinger, 1997). The extension is suggested to be related to both slab rollback and subduction processes, as well as due to the extrusion of the Anatolian Plate (McKenzie, 1972,

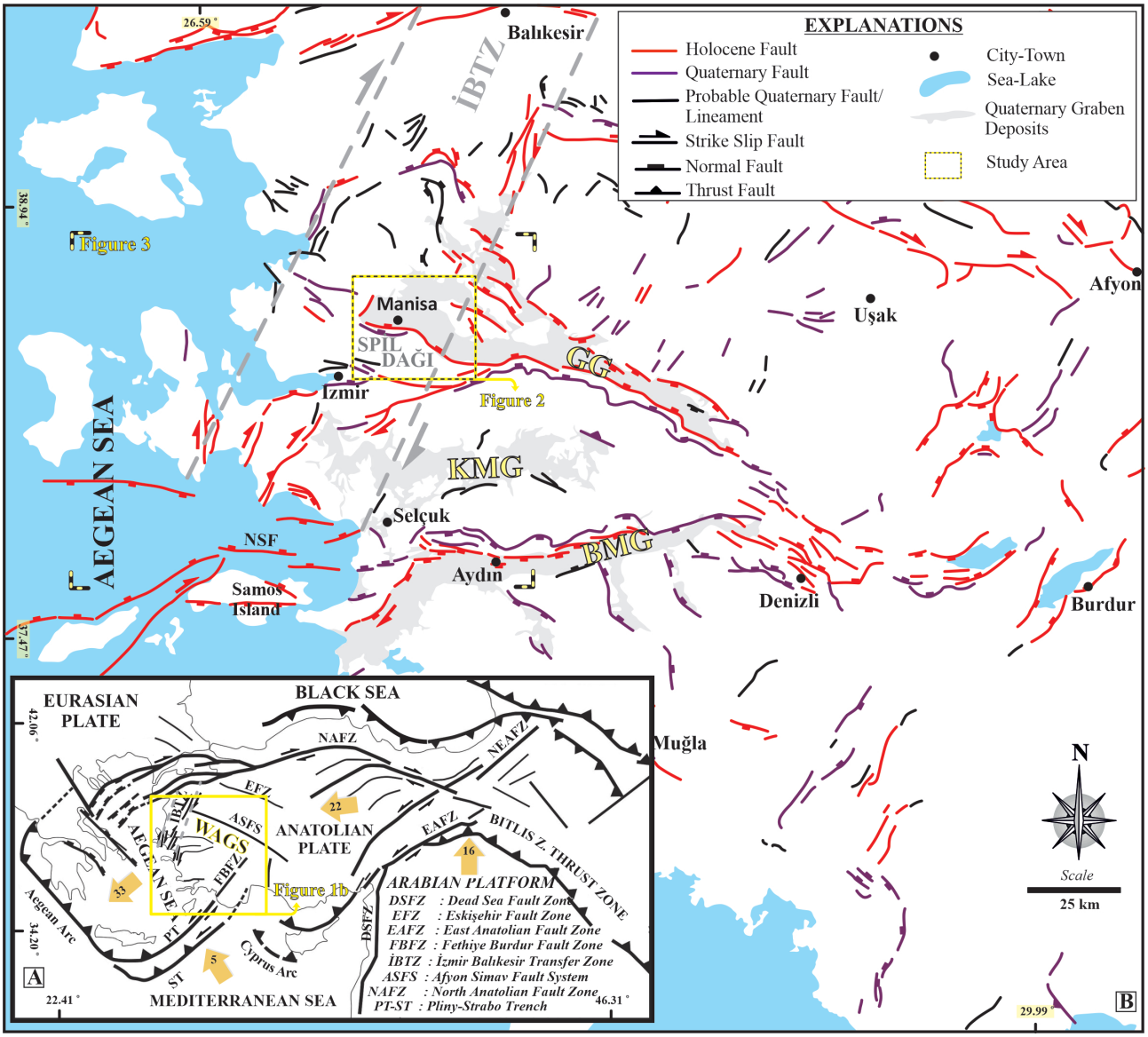


Figure 1. A: Overview map of the main tectonic features of Anatolia, after Gürer et al. (2004) and Uzel et al. (2015) with modifications. Yellow arrows show relative plate motions with numbers indicating rates in mm/year (Reilinger et al., 2006). WAGS: Western Anatolian Graben System. B: Simplified map showing active faults and major grabens of Western Anatolia (active faults redrawn from Emre et al., 2011, 2018). Offshore faults were modified from Lykousis et al. (1995), Ocakoğlu et al. (2005), Chamot-Rooke and Dotmed Working Group (2005), and Chatzipetros et al. (2013). GG: Gediz Graben, KMG: Küçük Menderes Graben, BMG: Büyük Menderes Graben, NSF: North Samos Fault.

1978; Şengör et al., 1985; Royden, 1993) along the North Anatolian Fault Zone (NAFZ) and East Anatolian Fault Zone (EAFZ). The westward extrusion of the Anatolian Plate is rotated anticlockwise toward the SW when it encounters the İzmir Balıkesir Transfer Zone (İBTZ), which accommodates differential extensional strain within the Aegean extensional system (Kaya, 1979; Ketin, 1948; McKenzie, 1972; Dewey and Şengör, 1979; Okay and Siyako, 1991; Ring et al., 1999; Sözbilir et al., 2003; Erkül et al., 2005; Sözbilir et al., 2007; Özkaymak and Sözbilir, 2008; Uzel and Sözbilir, 2008).

The İBTZ contains secondary strike-slip faults striking generally NE-SW and NW-SE, and normal faults striking E-W, all of which are seismically active and control the western edge of the grabens, such as Gediz Graben (GG), Küçük Menderes Graben (KMG), and Büyük Menderes Graben (BMG) (e.g., Uzel and Sözbilir, 2008; Sözbilir et al., 2011; Özkaymak et al., 2013; Uzel et al., 2015; Sümer,

2015; Softa, 2022) and a few studies evaluated the graben-bounding faults from a geomorphological perspective (e.g., Özkaymak and Sözbilir, 2012; Topal 2019a,b; Softa, 2022) (Figure 1b).

2.1. The Manisa Fault

The Manisa Fault (MF) forms the southwestern part of the southern margin of GG. MF is composed of two main active segments with lengths of 35 km and 26 km (Emre et al., 2018), and the north-dipping normal fault scarps are clearly visible to the unaided eye. These scarps separate Quaternary alluvial and colluvial deposits from carbonates belonging to the Late Cretaceous-Paleocene Bornova Flysch Zone (e.g., Bozkurt and Sözbilir, 2006; Özkaymak and Sözbilir, 2008) (Figure 2).

Analysis of the kinematics and Quaternary characteristics of the MF have been extensively studied over a number of years to evaluate its role in regional tectonics under an extensional regime (e.g., Weismantel, 1891; Sieberg, 1932; Pınar and Lahn, 1952; Oğuz, 1966; Ketin, 1968; Allen, 1974; Hancock and Barka, 1987; Şengör, 1987; Stewart and Hancock, 1988; Paton, 1992; Hakyemez et al., 1999; Emre et al., 2005; Bozkurt and Sözbilir, 2006; Özkaymak and Sözbilir, 2008; Emre et al., 2011; Özkaymak et al., 2011; Akçar et al., 2012; Temiz, 2012; Özkaymak and Sözbilir, 2012; Özkaymak et al., 2013; Emre et al., 2013; Emre et al., 2018; Duran et al., 2021; Mozafari et al., 2021).

According to paleo stress data from Bozkurt and Sözbilir (2006) and Özkaymak et al. (2011), MF is defined as a reactivated structure in which the final movement is in a NE-SW-oriented extension since approximately 300 ka from U-Th dating of calcite veins (Temiz, 2012). Moreover, triangular surfaces and geomorphic indices along the MF reflect the Quaternary activity of the fault (Özkaymak and Sözbilir, 2012). Furthermore, these authors calculated the

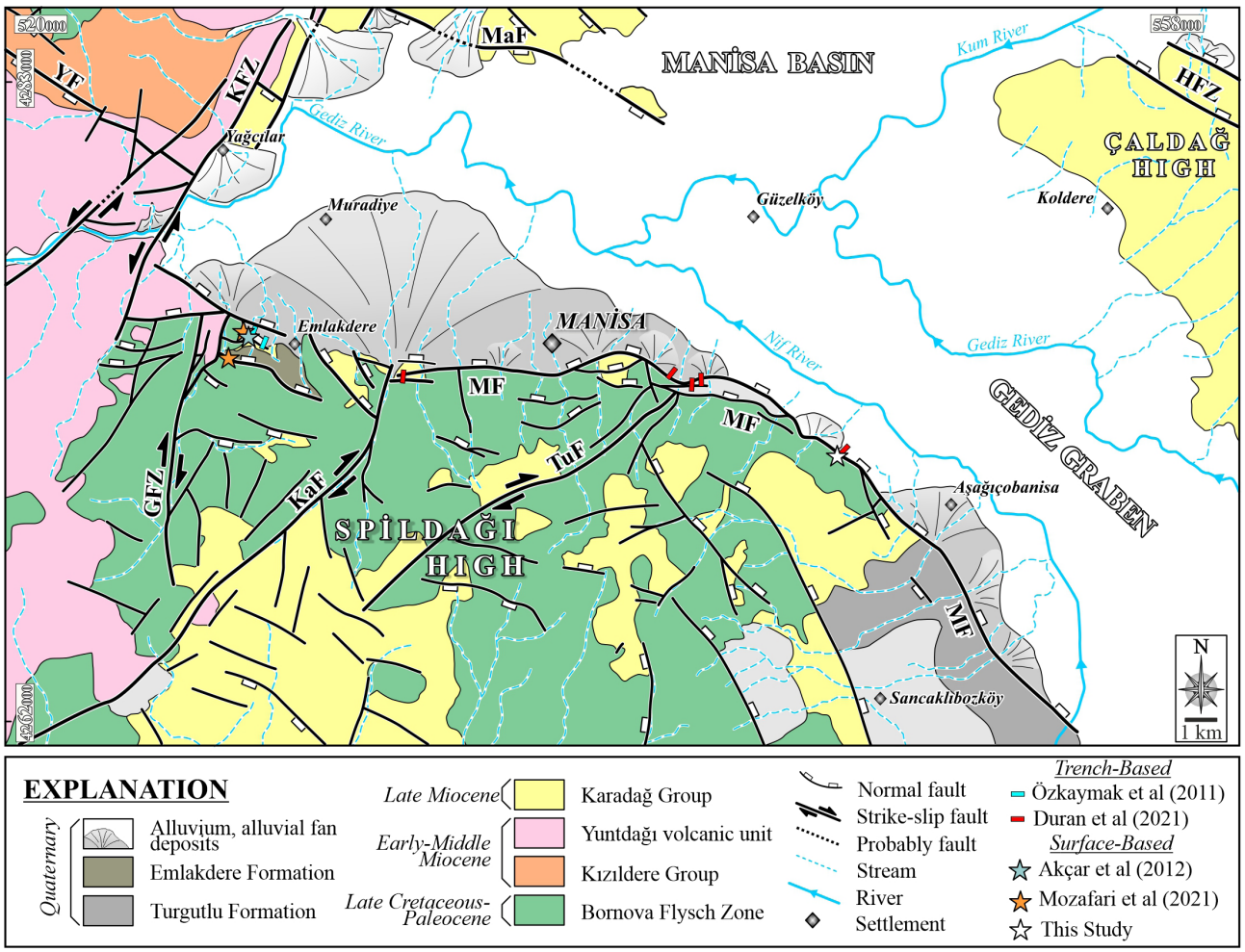


Figure 2. Geological map of the northern margin of Spil Dağı and its surroundings (revised from Özkaymak et al., 2013; Özkaymak and Sözbilir, 2012; Duran et al., 2021). The published paleoseismology locations are compiled from Özkaymak et al. (2011), Akçar et al. (2012), Duran et al. (2021) and Mozafari et al. (2021). MF, Manisa Fault; HFZ, Halitpaşa Fault Zone; KaF, Karaçay Fault; TuF, Turgutalp Fault; GFZ, Gürle Fault Zone; MaF, Maltepe Fault; KFZ, Kaleköy Fault Zone.

annual slip rate using the geomorphic indices and indicated that a differential uplift varying between 0.1 mm/year and 0.3 mm/year was recorded throughout the length of the fault.

From analysis of historical and instrumental catalogs it is clear that numerous severe earthquakes occurred on normal faults concentrated in the Western Anatolia region (e.g., Soysal et al., 1981; Guidoboni et al., 1994; Ambraseys, 2009; Kadirioglu et al., 2017; KOERI, 2022) (Figure 3). Although the exact location of epicenters of historical earthquakes are not precisely known, significant earthquakes were listed between 17AD and 1862 AD for the GG and MF region (e.g., Ergin et al., 1967; Ambraseys and Finkel, 1995; Ambraseys and Jackson, 1998; Başarır Baştürk et al., 2017).

Figure 3 shows the distribution of epicenters around the MF. The distribution of earthquakes, which is based on the earthquake catalog of Boğaziçi University, Kandilli Observatory and Earthquake Research Institute (KOERI), span from 26 BC to the present day. The location of the historically inferred epicenters are a significant distance from the deformation area observed in the field today, although the word "Manisa" is mentioned in the catalog in which the earthquakes are documented. As shown in Figure 3, this deformation area offers a pattern compatible with Western Anatolian seismicity in terms of microearthquake activity. There is no evidence of magnitude of 6-7earthquakes in the instrumental period in this deformation area. There are only 3 earthquakes that correspond to a range in magnitude of 5-6, including those of forced association.

3. Methodology

3.1. Site selection and sample preparation

Luminescence depth profiles measured above and below the present-day surface on bedrock fault scarps are a

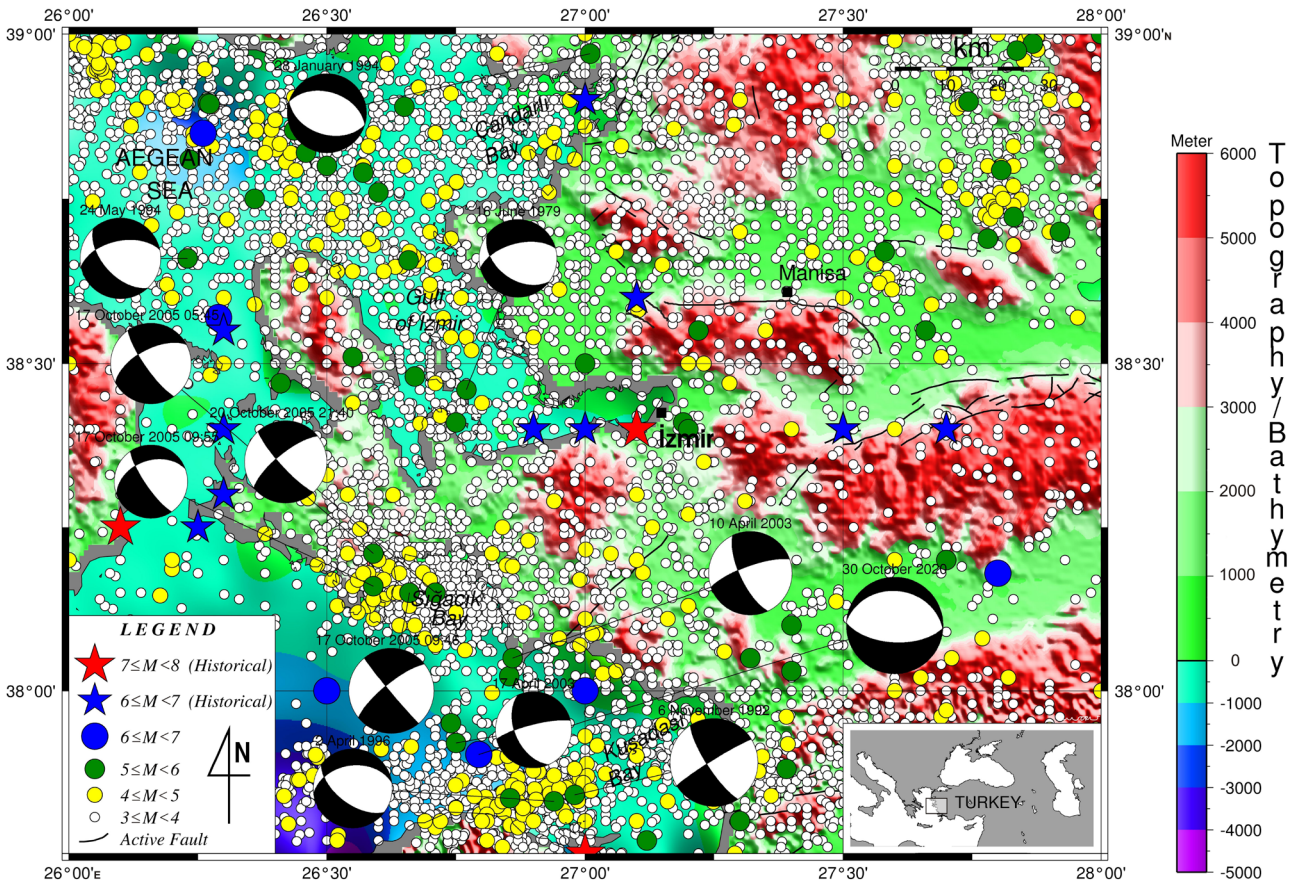


Figure 3. Map of epicenter distribution for İzmir and surroundings in the period 26BC to present year (2022) from earthquakes of magnitude 3.0 and greater, from the electronic earthquake catalog of the Boğaziçi University Kandilli Observatory and Earthquake Research Institute (KOERI)[1], with comparison to the simplified fault system of the region. Active faults are modified from Emre et al. (2013). The map was generated using GMT (Wessel and Smith, 2006). Topography and bathymetry data are from USGS.[2]

[1] KOERI (Kandilli Observatory and Earthquake Research Institute), Boğaziçi University, Electronic Earthquake Catalogue, Recent Earthquakes in Turkey [online]. Website http://www.koeri.boun.edu.tr [accessed June 13, 2022].

[2] USGS (United States Geological Survey). Website http://neic.usgs.gov [accessed January 4, 2007].

unique approach to acquire long timescales with sufficient detail to observe temporal variations in slip. The acquisition of robust data is directly dependent on the selection and characterization of sampling localities. Therefore, in the first part of the methodology, we performed extensive fieldwork to identify and characterize sampling sites. Initial fieldwork was staged based on remote sensing work utilizing existing active fault maps, geological maps, and satellite imagery.

We conducted a field reconnaissance and sampling studies in early August 2019 in order to have samples to process over the winter, followed by another field study to take calibration samples in October 2021. Sampling localities were selected on the basis that the bedrock fault scarp has only been exposed because of earthquake rupture, and not due to any sedimentary modification. Weathering exerts a strong control on breaking down bedrock fault scarps; thus, post-LGM climate is preferable for good preservation of scarps. Eight samples were collected from the exposed surface of the MF along the route parallel to slip lines. To obtain a record throughout the paleoseismological history of the MF, samples were collected from in situ bedrock above and below the present-day surface. To collect samples below the present-day surface, we used the excavated trench (Trench number 3, Duran et al., 2021) located in front of the MF scarp. Samples were collected using a portable water-cooled diamond-tipped coring drill, utilizing climbing equipment on the fault plane (Figure 4).

Measurement protocols and sample preparation for surface exposure dating are less established compared to conventional sediment luminescence dating and it is also dependent on the sample lithology. Therefore, similar sample preparation and measurement protocols as indicated by Sohbati et al. (2011, 2012a, b) have been subjected to the samples. More detailed information about the application methodology of the technique can be found in mentioned studies. The MF fault plane is composed of calcite crystals, so procedures were modified for preparation of calcite grains. To measure OSL-depth profiles, cores (30 mm diameter, >20 mm in length) were sampled using the coring drill. The cores were sliced in 1 mm increments using a diamond-tipped wafering blade (0.3 mm thick) mounted on a Buehler Isomet high-precision low-speed water-cooled saw at the İzmir Institutes of Technology Department of Conservation and Restoration of Cultural Heritage. The slices were gently crushed with a mortar and pestle and the resulting grains were sieved to retain those with a diameter of 90–250 μm at Dokuz Eylül University Department of Geology. The grains were washed in weak (1%) HCl acid (Huang et al., 2022) for 2 min to remove the outer surface layer, as crushing procedures may have induced lattice defects in the surface layer which could produce a spurious thermoluminescence (TL) signal (Wintle 1975, 1978) but may also effect OSL signals (e.g., Schmitt et al., 2011). The prepared mineral grains were mounted on 10-mm diameter stainless steel discs (approximately 50 grains per aliquot).

3.2. Luminescence measurement

Luminescence characteristics of each slice and related measurements were precisely measured under specially equipped laboratory conditions at Ankara University Luminescence Dating Research Laboratory (AU-LDRL).

All luminescence measurements were conducted using a Risø TL/OSL reader (model TL-DA 20) with blue stimulation (λ = 470 nm, approximately 80 mW/cm^2) and UV detection with a 7.5 mm Hoya U-340 filter. The luminescence reader is equipped with a ^{90}Sr/^{90}Y calibrated beta radiation source for on-plate irradiation, delivering a dose rate of approximately 0.1 Gy/s on stainless steel discs. The heating rate was selected as 5 °C/s for all heat treatments, carried out in a nitrogen gas atmosphere. The natural OSL signal, L_x, and the following test dose response, T_x, were measured in the first cycle of a single-aliquot regenerative-dose (SAR) protocol (Murray and Wintle, 2000) for each of the aliquots. A preheat of 200 °C for 10 s and cut-heat of 180 °C were applied to natural and test doses, respectively. For calculations, the net OSL signal was obtained by taking the initial 5s integral of the luminescence signal and subtracting the following 5s (as a background) to minimize contributions of unwanted components (more difficult to bleach and more thermally unstable) within the luminescence signal as indicated by Cunningham and Wallinga (2010).

3.3. Optically stimulated luminescence (OSL) fault scarp dating

The emerging OSL surface technique has the potential to address significant questions in the field of geosciences. One such new application is constraining the timing of paleoseismic activity on fault scarps. These sites are bedrock outcrops, where the rock bodies on either side of a fault plane systematically move when an earthquake occurs. When an earthquake happens at a site, a fresh rock surface is exposed and the "OSL-exposure clock" starts, and thus key targets for dating using an OSL fault scarp dating technique.

The OSL signal from mineral grains (typically quartz or feldspar) is routinely used to determine the elapsed time for which sediment grains were buried since sedimentary deposition. On the other hand, recent studies have shown that OSL dating can also be used to determine the duration of daylight exposure for rock surfaces (e.g., Laskaris and Liritzis, 2011; Sohbati et al., 2011, 2012a; Lehman et al., 2018; Gliganic et al., 2019). This novel approach provides complementary information for surface exposure dating



Figure 4. Sampling stages of the Manisa Fault scarp surface. A: A field view of the Manisa Fault scarp with the sampling area behind trench 3 of Duran et al. (2021); view toward the south. B: Calibration sample location at the sampled scarp; view toward the south. C-D-E: Surface examination processes (weathering bands, extensional cracks, and slip lines) prior to sampling; view toward the northwest. A coring drill with rock-climbing equipment was used for sampling.

using CRN. Furthermore, OSL surface exposure dating is applicable to younger timescales (approximately 10^{-4}–10^{4} year), (Sohbati et al., 2012a). The CRN dating signal develops over a few 100cm of material and is applicable over relatively older timescales (approximately 10^{2}–10^{6} year) (e.g., Gliganic et al., 2019). For proposed calibration study, importantly the two techniques overlap in the 10^{2}–10^{4} years range. The OSL surface exposure dating approach is based upon the depth-dependence of bleaching of the latent luminescence signal when exposed to daylight. The

dependence of the OSL signal on depth profile as well as exposure time is expressed with a double exponential function, as indicated by Sohbati et al.(2011, 2012a,b):

$$L = L_0 e^{-\sigma\varphi_0 t e^{-\mu x}} \quad (1)$$

where L is the OSL signal measured at depth x (mm) after exposure time t (s) and L_0 is the luminescence signal in field saturation. $\sigma\varphi_0$ (s^{-1}) is the effective detrapping rate constant describing an integral of the product of the wavelength-dependent photoionization crosssection (σ, cm^2) and photon flux at the rock surface (φ_0, $cm^{-2}s^{-1}$). μ (mm^{-1}) is the attenuation coefficient characterizing light penetration into the rock. As indicated by Sohbati et al. (2011) and Gliganic et al. (2019), this novel technique depends upon the first-order kinetics of the luminescence mechanism and an exponential attenuation of light intensity with depth. Additionally, it predicts that the longer the exposure duration, the deeper the bleaching of the luminescence signal into the rock surface. Therefore, there exists chronological information in the luminescence-depth profile. However, the assessment of daylight exposure time requires an independent knowledge of the $\sigma\varphi_0$ parameter, which is challenging to quantify from first principles (Sohbati et al., 2011, 2012a,b; Lehman et al., 2018; Gliganic et al., 2019). Among these researchers, Gliganic et al. (2019) has introduced a practical solution to quantify the $\sigma\varphi_0$ and μ parameters with the use of a calibration sample of known age, with similar lithological characteristics and light exposure conditions as the dating sample. For this purpose, we used a calibration sample chosen from a fresh fault scarp surface that was exposed from the first field survey in August 2019 to the second field survey in October 2021, equivalent to an exposure time of 749 days (approximately 2 years).

Modeling of the bleaching of the luminescence signal in this study has been carried out following a similar approach to Polikreti et al. (2002) and Lehmann et al. (2018), i.e. assuming the rock surface is continuously exposed to sunlight over the day. Hence, OSL signal bleaching is anticipated to transmit deeper into the rock surface following the elapsed daylight duration, which is demonstrated schematically in Figure 5.

4. Findings

According to the reference sample, the calibrated OSL surface dating results are shown in Table 1. For each sample the L_x/T_x (sensitivity corrected natural OSL signal) data for each slice were plotted against depth (Figure 6).While the measured OSL signals were negligible at 1 mm depth, it was observed that the signals increased with depth and the signal saturation was stable at a depth of 6-7 mm (Figure 7). A few minutes to a few hours of daylight exposure is sufficient to bleach versus the depth of rocks (Habermann et al., 2000; Vafiadou et al., 2007; Sohbati et al., 2011, 2012a,b). It is shown that our results are comparable with their luminescence signals with exposure time within the depth (Figure 7).

Although there is no clearly defined mathematical function in the literature, there are different approaches based on the above-mentioned equation (Eq. 1). Therefore, in this study, the bleaching with depth model equation as shown by Sohbati et al. (2012a) was used for the mathematical fitting approach. For this purpose, the OSL points were fitted with the bleaching signals with the equation (Eq.1) using the software OriginLab to determine the likelihood of the surface rupture earthquake events. For error calculations of ages, as shown in Table 1, the compatibility of OSL results with mathematical fit parameters to the bleaching model was taken into account. For this purpose, the OSL points in the related graphs (Figures 6 and 7) yield the average of at least three aliquots for each depth. Parameters of μ and $\sigma\varphi_0$ were determined using the global fit function and its iterations. The function is based on the depth profile for effective bleaching rate and uses goodness-of-fit parameters to determine a robust scarp date. According to function outputs, parameters of μ and $\sigma\varphi_0$are 0.79 ± 0.12 and 1×10^{-7}, respectively. From this point on, the fitted bleaching signals of all samples are presented in Table 1. According to preliminary findings, based on the luminescence parameters of calibration and other samples are evaluated together, our data indicates that a six-earthquake cycle has occurred at 65 ± 22 year (LSD1), 154± 22 year (LSD3), 416 ± 48 year (LSD4), 1103 ± 82 year (LSD5), 2067 ± 138 year (LSD6), 5376 ± 48 year (LSD7), and 6432 ± 218 year (LSD8).

5. Discussion and concluding remarks

Western Anatolia has experienced several approximately Mw 6 earthquakes causing damage and loss of life over the past several decades and, with geodetic estimates of fast extension rates, the seismic hazard is potentially significant. Despite this, there are only a few studies that have investigated the timing of faulting in Western Anatolia (using CRN methods), and few estimates of Quaternary fault slip rates exist for the region. Hitherto the OSL surface dating technique has not been used to study faults in these regions. In this novel research, a critical aspect is to the identification of calibration sites to compare luminescence and other dating results on the same fault surface.

OSL fault scarp dating strongly depends on a calibration sample to adapt the depth profile of coefficient factors ($\sigma\varphi_0$ and μ) in the same lithology to the sampled surfaces. To calibrate or test the OSL surface results, either the known age of the surface should be used (e.g., Softa et al., 2022; Luo et al., 2022), or CRN dating studies must be carried out.

For this purpose, the bleaching profiles obtained from fault surfaces, the $\sigma\varphi_0$ and μ parameters for each

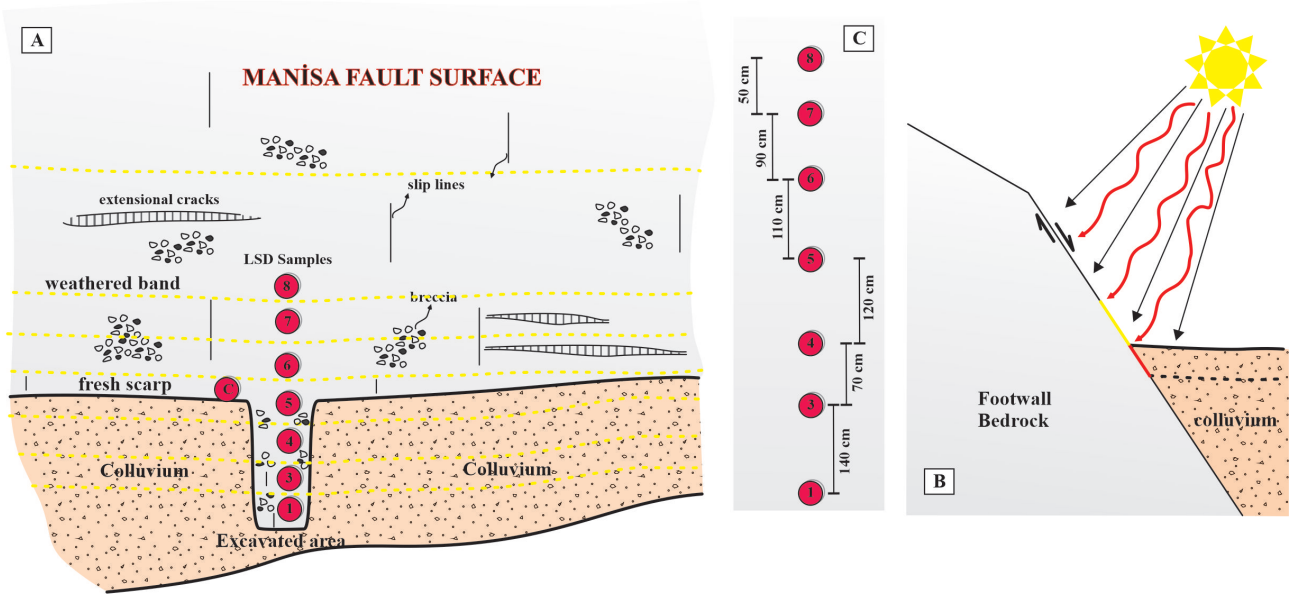


Figure 5. A schematic sketch of the Manisa Fault scarp. A: Photo shows important parameters (e.g., weathering bands, extensional cracks, and slip lines) for the sampling process. B: Conceptual model for the mechanism of the OSL surface dating applied to the fault scarp. Note that the samples were collected from the fresh and weathered rock surface that was exposed after the earthquakes. C: Plan of the sample locations along the Manisa Fault scarp.

Table 1. Results for model outputs based on the bleaching luminescence-depth profile applied to the Manisa Fault scarp. PS: present surface, BS: below surface, AS: above surface.

Sample code	Scarp height (cm)		$\sigma\varphi_0$	μ	Calibrated age (year)	Corresponding earthquakes
LSD-1	−330	BS	3.24×10^{-9}	0.79± 0.12	65 ± 22	*-
LSD-3	−190		6.23×10^{-10}		154 ± 22	1862 AD
LSD-4	−120		2.17×10^{-10}		416 ± 48	1595 AD
LSD-5	0 (PS)		3.89×10^{-10}		1103 ± 82	926 AD
LSD-6	110	AS	4.85×10^{-11}		2067 ± 138	17AD
LSD-7	200		7.28×10^{-11}		5376 ± 289	**-
LSD-8	250		1.15×10^{-10}		6432 ± 218	**-
Calibration			1×10^{-7}		2	

surface are expected to be similar to the calibration sample. A value of the light attenuation parameter μ and effective detrapping rate $\sigma\varphi_0$are 0.79 ± 0.12 and 1×10^{-7} using the calibration sample, respectively. Although the effective detrapping rate of the fault surface theoretically is expected to be the same for all samples, it is found that the rate ranges between 10^{-7} and 10^{-11} (Table 1). As stated by Sohbati et al. (2012a,b), Meyer et al. (2018) and, Lehmann et al. (2018), this discrepancy can arise from a deviation of the incident solar spectrum, variable mineralogy, and differential photon flux penetration throughout the scarp. Meyer et al. (2018) has also noted that the μ value might spatially diverge with depth across the rock within large heterogeneous crystals. In addition to that, it can also be associated with local shadow effects due to local fluctuating climatic conditions.

Nevertheless, we obtain the same effective photoionization crosssection (σ) and light attenuation coefficient (μ) values for all scarp samples, and the photon flux (φ_0) at the faulted surface is regionally similar. Although the $\sigma\varphi_0$ values differ slightly for our samples, our results show that it is likely that the attenuation characteristics of the fault scarp samples are typical, similar to the findings of Sohbati et al. (2012a,b).

The luminescence signals of calcite, especially for TL, are promising, although they have been previously

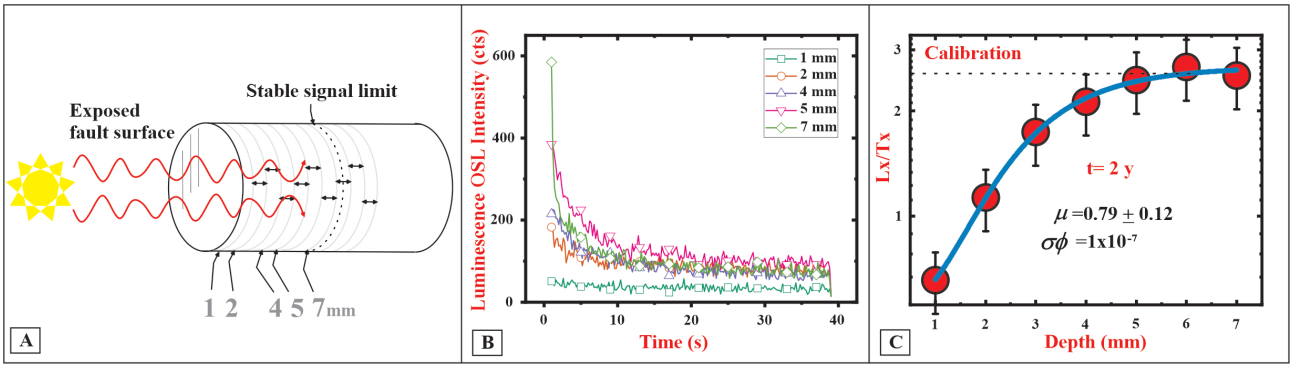


Figure 6. A: Schematic of the position of coring drill samples and indication of the possible stable signal limit with depth. B: Luminescence properties of the calibration sample and shine-down curves of the sample with depth profile. C: Bleaching signal depth profile of the calibration sample. Note that the calibration sample yields values of 0.79 ± 0.12 and 1×10^{-7} for parameters μ and $\sigma\varphi_0$, respectively.

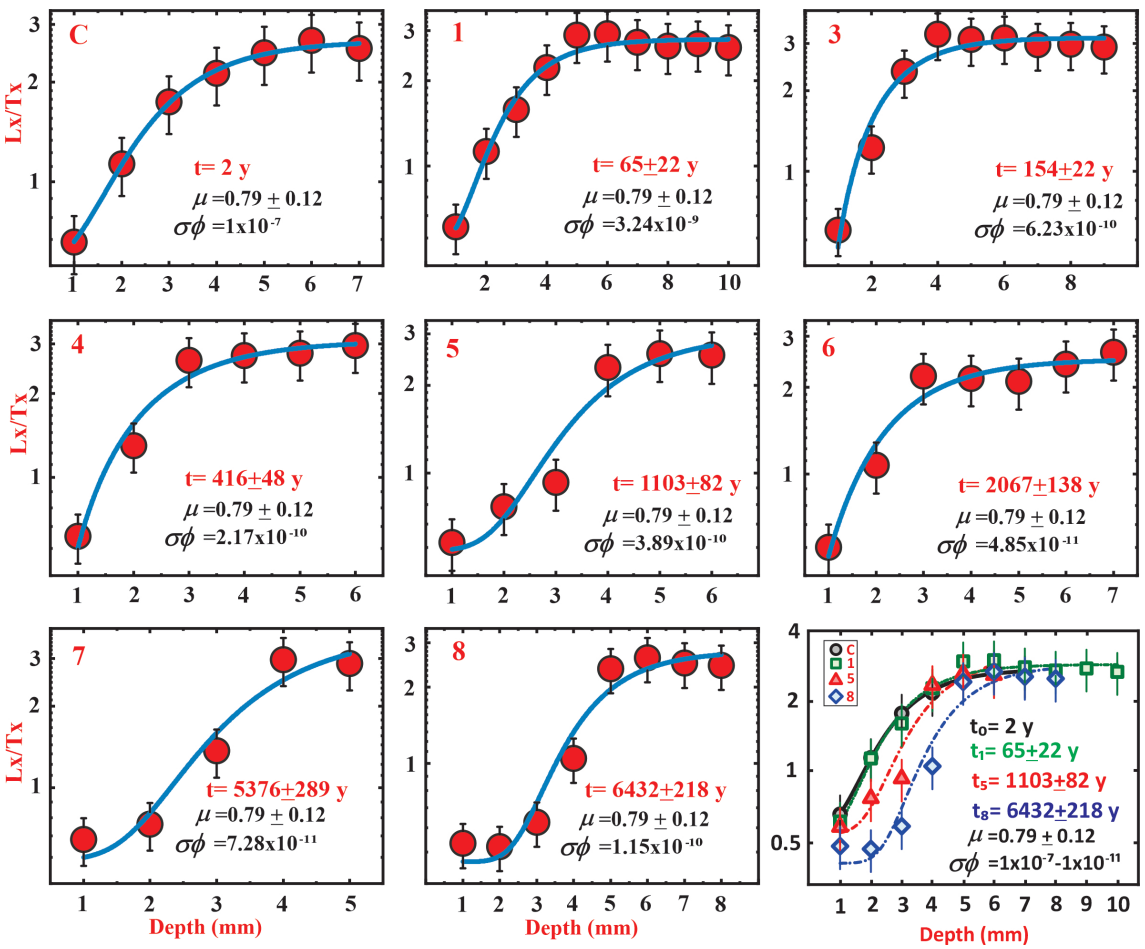


Figure 7. Signal depth profiles and results of curve fitting of the bleaching profiles from the calibration sample. C: Calibration samples. Numbers from 1 to 8 show the sampling code. The right bottom panel shows model fits for representative samples (C, 1, 5, 8).

described in the literature with controversial results. Various studies have shown that deconvolution methods can be used to separate components of luminescence signals from calcite to use in dating studies (Wintle, 1978; Debenham, 1983; Debenham and Aitken, 1984; Tatumi et al., 1989; Roque et al., 2001; Zhang and Wang, 2020; Şahiner et al., 2021). In this work, it is concluded that calcite samples have OSL signals that successfully

pass test measurements and can be used in OSL surface dating applications, which is promising in studies in this field. This study could be expanded and tested with calcite samples taken from different regions and could be comparatively supported by further studies with other dating techniques. It can be useful in areas where it is not possible to work with minerals such as quartz and feldspar, especially in carbonate-dominated regions. In addition, this study provides a basis for expanding the study area of luminescence dating applications. Although the results are preliminary and tested in the special geological field, the authors believe that the application of luminescence fault scarp dating using calcite minerals could be important for future studies.

From a methodological point of view, the preliminary results signify that the MF is responsible for at least six surface rupturing earthquakes since the Holocene which occurred at 65 ± 22 year (LSD1), 154± 22 year (LSD3), 416 ± 48 year (LSD4), 1103 ± 82 year (LSD5), 2067 ± 138 year (LSD6), 5376 ± 48 year (LSD7), and 6432 ± 218 year (LSD8). The first sample was taken from below the surface (LSD1) and was evaluated as postdating earlier earthquake events. Therefore, when a fresh surface is exposed after the relevant earthquake, this marker line is thought to be covered and reexposed to the daylight due to anthropogenic effects. Despite this underestimate on the first of the surfaces, the rest of the data are considered more precise for paleoseismological evaluation. Between LSD3 and LSD8the data are consistent with previous cosmogenic scarp dating and trench-based paleoseismological results (Figure 8).

CRN dating studies suggest that paleoseismological evaluations of the MF can be explained under two and single different scenarios (Akçar et al., 2012; Mozafari et al., 2021) using the different statistical MATLAB models such as those of Schlagenhauf et al. (2010) and Tikhomirov et al. (2019). Akçar et al. (2012) stated that two seismic events occurred on the MF, one at 13.7 ± 0.8 ka with a displacement of 0.5 ± 0.2 m and one at 7.8 ± 0.5 ka with 2.15± 0.35 m offset in the first scenario. Moreover, their second scenario reflects one seismic event at 8.6 ± 0.6 ka with 2.65 ± 0.35 m of slip. After their study, Mozafari et al. (2021) dated the MF surfaces with the same technique. They obtained three seismic events; the first at 6.5 ± 1.6 ka with a vertical displacement of 2.7 ± 0.4 m, and the second and third at 3.5 ± 0.9 ka, and 2.0 ± 0.5 ka with vertical displacements of 3.3 ± 0.5 m, and 3.6 ± 0.5 m, respectively.

To shed light on the slip rate, it is highly recommended that both the more continuous dense sampling throughout the surface and the more statistical evaluation using the luminescence package program (R) after will be written surface luminescence dating code.

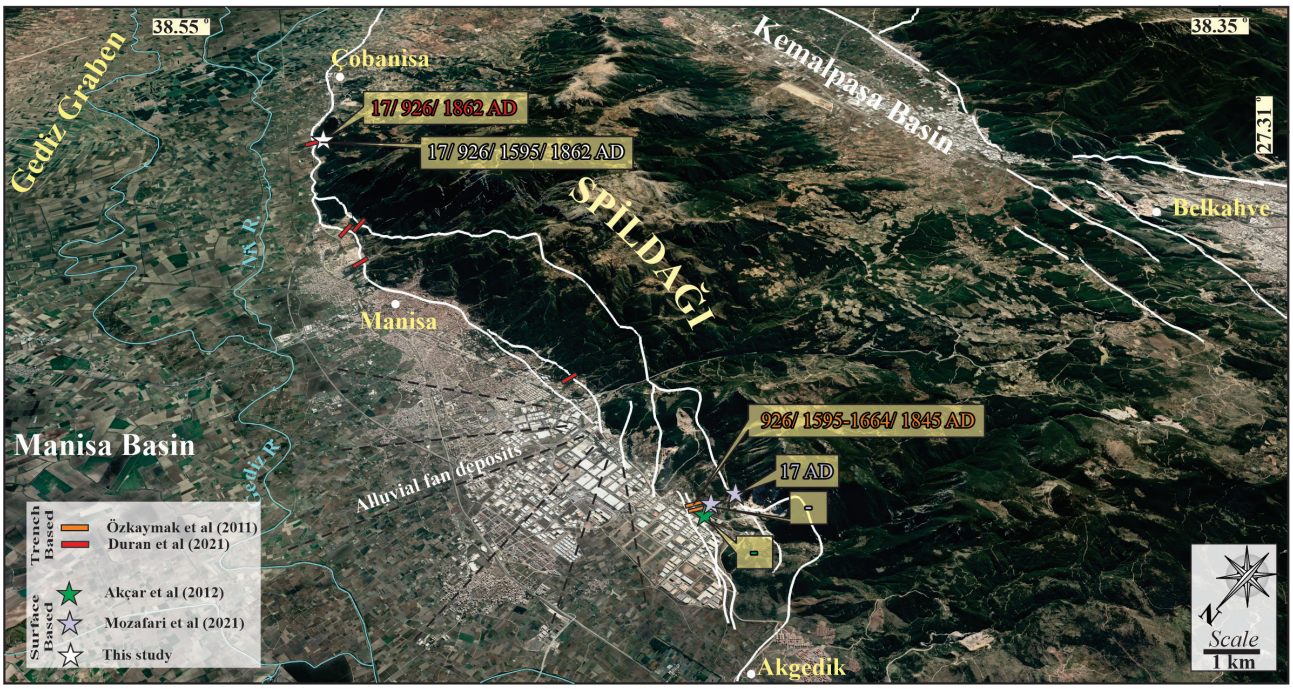


Figure 8. Comparison of first results of the OSL surface dating technique with previous paleoseismological studies on the Manisa Fault. The matching of historical earthquakes against chronologies are compiled from Özkaymak et al. (2011), Akçar et al. (2012), Duran et al. (2021) and Mozafari et al. (2021). The thick line in the box indicates that the observed chronologies have not been matched to the historical catalogs because the time interval of the catalog is limited. White lines indicate an active fault according to Emre et al. (2018).

Table 2. A comparison of the surface and trench based paleoseismological studies on the Manisa Fault in the Western Anatolia extensional system.

	Trench-based		Fault surface/scarp-based		
Manisa Fault	Özkaymak et al., 2011	Duran et al., 2021	Akçar et al., 2012	Mozafari et al., 2021	This study
Western segment	926 AD		17 AD	17 AD	
	1595 AD		926 AD		
	1664 AD		1862 AD		
	1845 AD				
Eastern segment		17 AD			17 AD
		926 AD			926 AD
		1862AD			1595 AD
					1862 AD

Western Anatolia is vulnerable to the high seismicity since the historical period, cosmogenic surface dating was applied to the fault surface in order to determine earthquake recurrence interval, the elapsed time since the most recent surface ruptured earthquake, Quaternary slip rate (Akçar et al., 2012; Mozafari et al., 2019a, 2019b; Gregory et al., 2020; Mozafari et al.,2021, 2022). While Akçar et al. (2012) and Mozafari et al. (2021) studied the western segment of the MF, there are no surface-based paleoseismology studies on the eastern segment of the MF, excluding trench based paleoseismology (Özkaymak et al., 2011; Duran et al., 2021), (Table 2). In addition, Akçar et al. (2012) stated that two of the 17 AD, 926 AD, and 1845 AD earthquakes seem to have produced ruptures on the western segment of the MF. Similarly, Mozafari et al. (2021) articulated that the 17 AD earthquake was responsible for the most recent surface ruptures on the western segment of the MF.

From these studies, Özkaymak et al. (2011) stated that there are three surface rupture events that can be associated with 926 AD, 1595/1664 AD, and 1845 AD historical earthquakes. Further, between 30.6 ± 8.8 ka and 0.1 ± 0.1 ka, six surface rupture events were articulated by Duran et al. (2021) in the eastern of the MF. According to their results within the five trenches, the 17 AD, 926 AD, and 1862 AD earthquakes overlapped with respect to historical earthquake catalogs. From these trench areas, Trench 3 which was excavated on the most eastern of the MF, reflected 926 AD and 1862 AD earthquakes within the four events starting from approximately 6.5 ka.

Because our study was carried out on the fault surface behind trench 3 of Duran et al. (2021), the observable events in trench 3 are expected to be similar to our own robust results. Our OSL surface results signify that a total of six surface rupture earthquakes occurred at 6.4 ± 0.2 ka (E1), 5.4 ± 0.1 ka (E2), 2.1 ± 0.1 ka (E3), 1.1 ± 0.1 ka (E4), 0.4 ± 0.1 ka (E5), and 0.2 ± 0.1 ka (E6) on the MF. The results in between LSD3 and LSD6 can be correlated with 17 AD (E3), 926 AD (E4), 1595 AD (E5) and 1862 AD (E6) with respect to historical earthquake catalogs. However, E1 and E2 events are not attributed to an exact earthquake due to the limited time interval of historical earthquake catalogs (Table 1).

Finally, from this point on, it is highly likely that the luminescence surface dating on the MF surface not only will add new data and information to the existing earthquake catalogs and is also possible to reveal the potential seismic threat for surrounding settlements.

Acknowledgments
This research is supported by Dokuz Eylül University, Scientific Research Project, project number of 2021. KB.FEN.017. This research project is also strictly evaluated and selected as an outstanding project by anonymous reviewers via Marie Sklodowska Curie Pre-Evaluation Support of TÜBİTAK with the project number of121U277. The authors would like to thank Dr. Elif Uğurlu Sayın who is the director of Material Conservation Laboratory at the İzmir Institutes of Technology Department of Conservation and Restoration of Cultural Heritage for gives opportunity to use the laboratory. Moreover, Eren Şahiner is a recipient of the distinguished young scientist award, which is a program of the Turkish Academy of Sciences (TÜBA-GEBİP 2021). The authors would like to thank the anonymous reviewers for their critical and constructive comments that greatly contributed to improving the final version of the paper.

References

Akçar N, Tikhomirov D, Özkaymak Ç, Ivy-Ochs S, Alfimov V et al. (2012). 36Cl exposure dating of paleoearthquakes in the Eastern Mediterranean: First results from the western Anatolian Extensional Province, Manisa fault zone, Turkey. GSA Bulletin 124(11-12): 1724-1735.

Akkar S, Kale Ö, Yakut A, Ceken U (2018). Ground-motion characterization for the probabilistic seismic hazard assessment in Turkey. Bulletin of Earthquake Engineering 16 (8): 3439-3463.

Aktuğ B, Parmaksız E, Kurt M, Lenk O, Kılıçoğlu A et al. (2013). Deformation of central anatolia: GPS implications. Journal of Geodynamics 67 (1): 78-96.

Aktuğ B, Tiryakioğlu İ, Sözbilir H, Özener H, Özkaymak Ç et al. (2021). GPS derived finite source mechanism of the 30 October 2020 Samos earthquake, Mw= 6.9, in the Aegean extensional region. Turkish Journal of Earth Sciences 30(SI-1): 718-737.

Allen CR (1974). Geological criteria for evaluating seismicity. Geological Society of America Bulletin 86: 1041-1057.

Ambraseys NN, Finkel CF (1995). The Seismicity of Turkey and adjacent areas: a historical review, 1500-1800, İstanbul, Muhittin Salih Eren.

Ambraseys NN, Jackson JA (1998). Faulting associated with historical and recent earthquakes in the Eastern Mediterranean region. Geophysical Journal International 133(2): 390-406.

Ambraseys N (2009). Earthquakes in the Mediterranean and Middle East: a multidisciplinary study of seismicity up to 1900. Cambridge University Press.

Banerjee D, Singhvi AK, Bagati TN, Mohindra R (1997). Luminescence chronology of seismites in Sumdo (Spiti valley) near Kaurik-Chango Fault, Northwestern Himalaya. Current Science 73: 276-281.

Banerjee D, Singhvi AK, Pande K, Gogte VD, Chandra BP (1999). Towards a direct dating of fault gouges using luminescence dating techniques - methodological aspects. Current Science 77: 256-268.

Barka AA, Reilinger R (1997). Active tectonics of the Mediterranean region: deduced from GPS, neotectonic and seismicity data. Annals of Geophysics XI: 587-610.

Basmenji M, Akyuz HS, Kirkan E, Aksoy ME, Ucarkus G et al. (2021). Earthquake history of the Yatagan Fault (Mugla, SW Turkey): implications for regional seismic hazard assessment and paleoseismology in extensional provinces. Turkish Journal of Earth Sciences 30(2): 161-181.

Başarır Baştürk N, Özel NM, Altınok Y, Duman TY (2017). Türkiye ve yakın çevresi için geliştirilmiş tarihsel dönem (MÖ 2000 – MS 1900) deprem Katalogu. Türkiye Sismotektonik Haritası Açıklama Kitabı, MTA Özel Yayınlar Serisi-35, 287 S. Ankara, 2016.

Benedetti L, Finkel R, Papanastassiou D, King G, Armijo R et al. (2002). Post-glacial slip history of the Sparta fault (Greece) determined by 36Cl cosmogenic dating: Evidence for non-periodic earthquakes. Geophysical Research Letters 29(8): 87-1.

Benedetti L, Finkel R, King G, Armijo R, Papanastassiou D et al. (2003). Motion on the Kaparelli fault (Greece) prior to the 1981 earthquake sequence determined from 36Cl cosmogenic dating. Terra Nova 15(2): 118-124.

Bingöl E (1976). Batı Anadolu'nun jeotektonik evrimi. MTA dergisi 86: 14-43.

Bozkurt E (2001). Neotectonics of Turkey-a synthesis. Geodinamica acta 14(1-3): 3-30.

Bozkurt E, Sözbilir H (2006). Evolution of the large-scale active Manisa Fault, Southwest Turkey: implications on fault development and regional tectonics. Geodinamica Acta 19(6): 427-453.

Bürgmann R, Segall P, Lisowski M, Svarc J (1997). Postseismic strain following the 1989 Loma Prieta earthquake from GPS and leveling measurements. Journal of Geophysical Research 102: 4933-4955.

Cunningham, A. C., Wallinga, J. (2010). Selection of integration time intervals for quartz OSL decay curves. Quaternary Geochronology 5(6): 657-666.

Campbell KW (1982). Bayesian analysis of extreme earthquake occurrences. Part I. Probabilistic hazard model. Bulletin of Seismological Society of America 72:1689-1705.

Campbell KW (1983). Bayesian analysis of extreme earthquake occurrences. Part II. Application to the San Jacinto fault zone of southern California. Bulletin of Seismological Society of America 73:1099-1115

Chamot-Rooke N, Dotmed Working Group (2005). DOTMED – Deep Offshore Tectonics of the Mediterranean: a synthesis of deep marine data in eastern Mediterranean, Mémoire de la Société géologique de France and American Association of Petroleum Geologists Numéro Special: 177, 64 pp, 9 maps.

Chatzipetros A, Kiratzi A, Sboras S, Zouros N, Pavlides S (2013). Active faulting in the north-eastern Aegean Sea Islands. Tectonophysics 597:106-122.

Civico R, Smedile A, Pantosti D, Cinti FR, De Martini PM et al. (2021). New trenching results along the İznik segment of the central strand of the North Anatolian Fault (Turkey): an integration with preexisting data. Mediterranean Geoscience Reviews 3(1): 115-128.

Debenham NC (1983). Reliability of thermoluminescence dating of stalagmitic calcite. Nature 304(5922): 154-156.

Debenham NC, Aitken MJ (1984). Thermoluminescence dating of stalagmitic calcite. Archaeometry 26(2): 155-170

Dewey JF, Şengör AC (1979). Aegean and surrounding regions: complex multiplate and continuum tectonics in a convergent zone. Geological Society of America Bulletin 90(1): 84-92.

Dikbaş A, Akyüz HS, Meghraoui M, Ferry M, Altunel E et al. (2018). Paleoseismic history and slip rate along the Sapanca-Akyazı segment of the 1999 İzmit earthquake rupture (Mw= 7.4) of the North Anatolian Fault (Turkey). Tectonophysics 738: 92-111.

Dikbaş A, Akyüz HS, Basmenji M, Kırkan E (2022). Earthquake history of the Gökova fault zone by paleoseismologic trenching, SW Turkey. Natural Hazards. https://doi.org/10.1007/s11069-022-05284-0

Ding YZ, Lai KW (1997). Neotectonic fault activity in Hong Kong: evidence from seismic events and thermoluminescence dating of fault gouge. Journal of the Geological Society, London 154: 1001-1007.

Dunai TJ (2010). Cosmogenic nuclides: principles, concepts and applications in the earth surface sciences. Cambridge University Press.

Duran I, Sözbilir H, Eski S, Softa M, Uytun H et al. (2021). Paleoseismic history of the Manisa fault zone, Western Anatolia. Turkish Journal of Earth Sciences 30 (SI-1): 806-832.

Emre Ö, Özalp S, Doğan A, Özaksoy V, Yıldırım C (2005). İzmir ve yakın çevresinin diri fayları ve deprem potansiyelleri. Jeoloji Etütleri Dairesi, Rapor No:10754 (in Turkish).

Emre Ö, Özalp S, Duman TY (2011). 1: 250,000 scale active fault map series of Turkey. İzmir (NJ 35-7) Quadrangle, Serial Number (6). General Directorate of Mineral Research and Exploration. Ankara, Turkey.

Emre Ö, Duman TY, Özalp S, Elmacı H, Olgun Ş et al. (2013). Active Fault Map of Turkey with an Explanatory Text [Açıklamalı Türkiye Diri Fay Haritası]. 1:1,250,000 Scale, General Directorate of Mineral Research and Exploration, Special Publication Series-30, Ankara.

Emre Ö, Duman TY, Özalp S, Şaroğlu F, Olgun Ş et al. (2018). Active fault database of Turkey. Bulletin of Earthquake Engineering 16 (8): 3229-3275. https://doi.org/10.1007/s10518-016 0041

Ergin K, Güçlü U, Uz Z (1967). Türkiye ve civarının deprem kataloğu, milâttan sonra 11 yılından 1964 sonuna kadar. TC, İstanbul Teknik Üniversitesi, Maden Fakültesi, Arz Fiziği Enstitüsü.

Erkül F, Helvaci C, Sözbilir H (2005). Evidence for two episodes of volcanism in the Bigadiç borate basin and tectonic implications for western Turkey. Geological Journal 40(5): 545-570.

Erturac MK (2021). Late Pleistocene-Holocene characteristics of the North Anatolian Fault at Adapazari Basin: evidence from the age and geometry of the fluvial terrace staircases. Turkish Journal of Earth Sciences 30(1): 93-115.

Fattahi M, Nazari H, Bateman, MD, Meyer B et al. (2010). Refining the OSL age of the last earthquake on the Dheshir fault, Central Iran. Quaternary Geochronology 5(2-3): 286-292. https://doi.org/10.1016/j.quageo.2009.04.005

Gliganic LA, Meyer MC, Sohbati R, Jain M, Barrett S (2019). OSL surface exposure dating of a lithic quarry in Tibet: Laboratory validation and application. Quaternary Geochronology 49: 199-204.

Gosse JC, Philips FM (2001). Terrestrial in situ cosmogenic nuclides: theory and application. Quaternary Science Reviews 20:1475–1560.

Gregory L, Goodall H, Uzel B, Sümer Ö, Softa M et al. (2020). Active faulting in western Turkey: the challenge of earthquake hazard estimation in a complex extensional regime based on cosmogenic isotope analyses. EGU General Assembly 2020, Online EGU2020-18658. https://doi.org/10.5194/egusphere-egu2020-18658

Guidoboni E, Comastri A, Traina G (1994). Catalogue of ancient earthquakes in the Mediterranean area up to the 10th century. Rome, Italy: Ist Naz Geofis.

Gurrola LD, Keller EA, Chen JH, Owen LA, Spencer JQ (2014). Tectonic geomorphology of marine terraces: Santa Barbara fold belt, California. Geological Society of America Bulletin 126: 219-233.

Gürer A, Bayrak M, Gürer ÖF (2004). Magnetotelluric images of the crust and mantle in the southwestern Taurides, Turkey. Tectonophysics 391(1):109-120

Habermann J, Schilles T, Kalchgruber R, Wagner GA (2000). Steps towards surface dating using luminescence. Radiation Measurements 32(5-6): 847-851.

Hakyemez HY, Erkal T, Göktas F (1999). Late Quaternary evolution of the Gediz and Büyük menderes grabens, western Anatolia, Turkey. Quaternary Science Reviews 18(4-5): 549-554.

Hancock PL, Barka AA (1987). Kinematic indicators on active normal faults in western Turkey. Journal of Structural Geology 9(5-6): 573-584.

Hu G, Yi CL, Zhang JF, Liu JH, Jiang T (2015). Luminescence dating of glacial deposits near the eastern Himalayan syntaxis using different grain-size fractions. Quaternary Science Reviews 124: 124-144.

Huang C, Zhang J, Wang L, Zhao H, Li SH (2022). Equivalent dose estimation of calcite using isothermal thermoluminescence signals. Quaternary Geochronology 70: 101310.

Ivy-Ochs S, Kober F (2008). Surface exposure dating with cosmogenic nuclides. E&G Quaternary Science Journal 57(1/2): 179-209.

Kadirioğlu FT, Kartal RF, Kılıç T, Kalafat D, Duman TY et al. (2017). Türkiye ve yakın çevresi için geliştirilmiş aletsel dönem (1900-2012) deprem kataloğu (M≥ 4, 0). Türkiye Sismotektonik Haritası Açıklama Kitabı (Ed. TY Duman). Maden Tetkik ve Arama Genel Müdürlüğü Özel Yayınlar Serisi-34, 1246.

Kaya O (1979). The (Neogene) stratigraphy and tectonics of the middle eastern Aegean depression. Bulletin of the Geological Society of Turkey 22: 35-58.

Ketin İ (1948). Uber die tektonisch-mechanischen Folgerungen aus den grossen anatolischen Erdbeben des letzten Dezenniums. Geologische Rundschau 36: 77-83 (in German).

Ketin İ (1968). Relations between general tectonic features and the main earthquake regions of Turkey. Bulletin of the Mineral Research and Exploration 71:63-67.

Kürçer A, Özaksoy V, Özalp S, Güldoğan ÇU, Özdemir E et al. (2017). The Manyas fault zone (southern Marmara region, NW Turkey): active tectonics and paleoseismology. Geodinamica Acta 29(1): 42-61.

Kürçer A, Özalp S, Özdemir E, Güldoğan ÇU, Duman TY (2019). Active tectonic and paleoseismologic characteristics of the Yenice-Gönen fault, NW Turkey, in light of the 18 March 1953 Yenice-Gönen Earthquake (Ms= 7.2). Bulletin of the Mineral Research and Exploration 159: 29-62. https://doi.org/10.19111/bulletinofmre.500553.

Kürçer A, Özdemir E, Olgun Ş, Özalp S, Çan T et al. (2021). Active tectonic and paleoseismological characteristics of the Dinar Fault, SW Anatolia, Turkey. Mediterranean Geoscience Reviews 3: 219-251. https://doi.org/10.1007/s42990-021-00052-x

Laskaris N, Liritzis I (2011). A new mathematical approximation of sunlight attenuation in rocks for surface luminescence dating. Journal of Luminescence 131(9): 1874-1884.

Le Pichon X, Angelier J (1979). The Hellenic arc and trench system: a key to the neotectonic evolution of the eastern Mediterranean area. Tectonophysics 60(1-2): 1-42.

Lee HK, Schwarcz HP (1994). Criteria for complete zeroing of ESR signals during faulting of the San Gabriel fault zone, southern California. Tectonophysics 235(4): 317-337.

Lee J, Spencer JQ, Owen LA (2001). Holocene slip rates along the Owens Valley fault, California: Implications for the recent evolution of the Eastern California Shear Zone. Geology 29 (9): 819-822.

Lehmann B, Valla PG, King GE, Herman F (2018). Investigation of OSL surface exposure dating to reconstruct post-LIA glacier fluctuations in the French Alps (Mer de Glace, Mont Blanc massif). Quaternary geochronology 44: 63-74.

Liritzis I (2011). Surface dating by luminescence: an overview. Geochronometria 38(3): 292-302.

Lukas S, Spencer JQ, Robinson RA, Benn DI (2007). Problems associated with luminescence dating of Late Quaternary glacial sediments in the NW Scottish Highlands. Quaternary Geochronology 2(1-4): 243-248.

Luo M, Chen J, Owen LA, Qin J, Yin J et al. (2022). A novel approach for reconstructing slip histories for bedrock fault scarps using rock surface luminescence dating. Geophysical Research Letters, e2022GL099526.

Lykousis V, Anagnostou C, Pavlakis P, Rousakis G, Alexandri M (1995). Quaternary sedimentary history and neotectonic evolution of the eastern part of Central Aegean Sea, Greece. Marine Geology 128(1-2):59-71.

McCalpin JP (2009). Application of paleoseismic data to seismic hazard assessment and neotectonic research. International Geophysics 95: 1-106. https://doi.org/10.1016/S0074 6142(09)95009-4.

McKenzie D (1972). Active tectonics of the Mediterranean region. Geophysical Journal International 30(2): 109-185.

McKenzie D (1978). Active tectonics of the Alpine-Himalayan belt: the Aegean Sea and surrounding regions. Geophysical Journal International 55(1): 217-254.

Meghraoui M, Atakan K (2014). The contribution of paleoseismology to earthquake hazard evaluations. In Earthquake Hazard, Risk and Disasters (pp. 237-271). Academic Press.

Meyer MC, Gliganic LA, Jain M, Sohbati R, Schmidmair D (2018). Lithological controls on light penetration into rock surfaces–Implications for OSL and IRSL surface exposure dating. Radiation Measurements 120: 298-304.

Mitchell SG, Matmon A, Bierman PR, Enzel Y, Caffee M et al. (2001). Displacement history of a limestone normal fault scarp, northern Israel, from cosmogenic 36Cl. Journal of Geophysical Research: Solid Earth 106(B3): 4247-4264.

Mozafari N, Sümer Ö, Tikhomirov D, Ivy-Ochs S, Alfimov V (2019a). Holocene seismic activity of the Priene–Sazlı Fault revealed by cosmogenic 36Cl, Western Anatolia, Turkey. Turkish Journal of Earth Sciences 28 (3): 410-437. https://doi.org/10.3906/yer-1810-6

Mozafari N, Tikhomirov D, Sumer Ö, Özkaymak Ç, Uzel B et al. (2019b). Dating of active normal fault scarps in the Büyük Menderes Graben (western Anatolia) and its implications for seismic history. Quaternary science reviews 220: 111-123.

Mozafari N, Özkaymak Ç, Tikhomirov D, Ivy-Ochs S, Alfimov V et al. (2021). Seismic Activity of the Manisa Fault Zone in Western Turkey Constrained by Cosmogenic 36Cl Dating. Geosciences 11(11): 451.

Mozafari N, Özkaymak Ç, Sümer Ö, Tikhomirov D, Uzel B et al. (2022). Seismic history of western Anatolia during the last 16 kyr determined by cosmogenic 36Cl dating. Swiss journal of Geosciences 115(1): 1-26.

Mukul M, Jaiswal M, Singhvi AK, (2007). Timing of recent out-of-sequence active deformation in the frontal Himalayan wedge: insights from the Darjiling sub-Himalaya, India. Geology 35: 999-1002.

Murray AS, Wintle AG (2000). Luminescence dating of quartz using an improved single aliquot regenerative-dose protocol. Radiation Measurements 33: 57-73.

Nas M, Lyubushin A, Softa M, Bayrak Y (2020). Comparative PGA-driven probabilistic seismic hazard assessment (PSHA) of Turkey with a Bayesian perspective. Journal of Seismology 24(6): 1109-1129.

Ocakoğlu N, Demirbağ E, Kuşçu İ (2005). Neotectonic structures in İzmir Gulf and surrounding regions (western Turkey): evidences of strike-slip faulting with compression in the Aegean extensional regime. Marine Geology 219(2-3):155-171.

Oğuz M (1966). Manisa Dağının Kuzey ve Kuzeybatısının Jeolojisi (Geology of the northern and Northwestern part of the Manisa Dag), Engl. summary: Fac. Sci. Ege Univ., Sci. Rept., no. 33, 20 p., İzmir.

Okay Aİ, Siyako M (1991).The new position of the İzmir-Ankara Neo-Tethyan suture between İzmir and Balıkesir (pp. 333-355). Ankara: Proceedings of the Ozan Sungurlu Symposium.

Owen LA, Finkel RC, Ma H, Spencer JQ et al. (2003). Timing and style of Late Quaternary glaciation in NE Tibet. Geological Society of America Bulletin 115 (11): 1356-1364.

Özaksoy V, Elmaci H, Özalp S, Kara M, Duman TY (2018). Holocene activity of the Orhaneli Fault based on palaoseismological data, Bursa, NW Anatolia. Bulletin of the Mineral Research and Exploration 156(156): 1-16.

Özkaymak Ç, Sözbilir H (2008). Stratigraphic and structural evidence for fault reactivation: the active Manisa fault zone, Western Anatolia. Turkish Journal of Earth Sciences 17: 615-635.

Özkaymak Ç, Sözbilir H, Uzel B, Akyüz HS (2011). Geological and paleoseismological evidence for late Pleistocene–Holocene activity on the Manisa Fault Zone, western Anatolia. Turkish Journal of Earth Sciences 20: 449-474.

Özkaymak Ç, Sözbilir H (2012). Tectonic geomorphology of the Spildağı high ranges, Western Anatolia. Geomorphology 173-174: 128-140.

Özkaymak Ç, Sözbilir H, Uzel B (2013). Neogene– Quaternary evolution of the Manisa Basin: Evidence for variation in the stress pattern of the İzmir-Balıkesir Transfer Zone, western Anatolia. Journal of Geodynamics 65: 117-135.

Palumbo L, Benedetti L, Bourles D, Cinque A, Finkel R (2004). Slip history of the Magnola fault (Apennines, Central Italy) from 36Cl surface exposure dating: evidence for strong earthquakes over the Holocene. Earth and Planetary Science Letters 225(1-2): 163-176.

Paton S (1992). Active normal faulting, drainage patterns and sedimentation in southwestern Turkey. Journal of the Geological Society of London 149:1031-1044.

Pavlides SB, Chatzipetros A, Tutkun ZS, Özaksoy V, Doğan B (2006). Evidence for late Holocene activity along the seismogenic fault of the 1999 Izmit earthquake, NW Turkey. Geological Society of London Special Publications 260(1): 635-647.

Pınar N, Lahn E (1952). Türkiye depremleri izahli katalogu. Bayındırlık Bakanlığı, Yapı ve İmar İşleri Reisliği Yayınları, Türkiye: 36 (6) (in Turkish).

Pisarenko VF, Lyubushin AA, Lysenko VB, Golubeva TV (1996). Statistical estimation of seismic hazard parameters: maximum possible magnitude and related parameters. Bulletin of Seismological Society of America 86:691-700.

Polikreti K, Michael CT, Maniatis Y (2002). Authenticating marble sculpture with thermoluminescence. Ancient TL 20: 11-18.

Porat N, Levi T, Weinberger R (2007). Possible resetting of quartz OSL signals during earthquakes - evidence from late Pleistocene injection dikes, Dead Sea Basin, Israel. Quaternary Geochronology 2: 272-277.

Prentice CS, Kendrick K, Berryman K, Bayasgalan A, Ritz JF et al. (2002). Prehistoric ruptures of the Gurvan Bulag fault, Gobi Altay, Mongolia. Journal of Geophysical Research 107 (B12): art. No. 2321.

Preusser F, Degering D, Fuchs M, Hilgers A, Kadereit A et al. (2008). Luminescence dating: basics, methods and applications. E&G Quaternary Science Journal 57 (1/2): 95-149. https://doi.org/10.3285/eg.57.1-2.5

Reilinger R, McClusky S, Vernant P, Lawrence S, Ergintav S et al. (2006). GPS constraints on continental deformation in the Africa-Arabia-Eurasia continental collision zone and implications for the dynamics of plate interactions. Journal of Geophysical Research: Solid Earth 111(B5).

Reilinger R, McClusky S, Paradissis D, Ergintav S, Vernant P (2010). Geodetic constraints on the tectonic evolution of the Aegean region and strain accumulation along the Hellenic subduction zone. Tectonophysics 488(1-4): 22-30.

Rhodes EJ (2011). Optically stimulated luminescence dating of sediments over the past 200,000 years. Annual Review of Earth and Planetary Sciences 39: 461-488.

Ring U, Laws S, Bernet M (1999) Structural analysis of a complex nappe sequence and late-orogenic basins from the Aegean Island of Samos, Greece. Journal of Structural Geology 21: 1575-1601.

Rittenour TM (2008). Luminescence dating of fluvial deposits: applications to geomorphic, palaeoseismic and archaeological research. Boreas 37(4): 613-635.

Roque C, Guibert P, Vartanian E, Bechtel F, Schvoerer M (2001). Thermoluminescence-dating of calcite: study of heated limestone fragments from Upper Paleolithic layers at Combe Sauniere, Dordogne, France. Quaternary Science Reviews 20(5-9): 935-938.

Royden L (1993). Evolution of retreating subduction boundaries formed during continental collision. Tectonics 12: 303- 325.

Schildgen TF, Robinson RAJ, Savi S, Phillips WM, Spencer JQG et al. (2016). Landscape response to late Pleistocene climate change in NW Argentina: Sediment flux and cosmogenic landslide signatures modulated by basin geometry. Journal of Geophysical Research Earth Surface 121: 392-414.

Schlagenhauf A, Gaudemer Y, Benedetti L, Manighetti I, Palumbo L et al. (2010). Using in situ Chlorine-36 cosmonuclide to recover past earthquake histories on limestone normal fault scarps: a reappraisal of methodology and interpretations. Geophysical Journal International 182(1): 36-72.

Schmidt C, Kreutzer S, Fattahi M, BaileyR, Zander A et al. (2011). On the luminescence signals of empty sample carriers. Ancient TL 29(2): 65-74.

Sieberg A (1932). Erdbebengeographie. Handbuch der Geophysik, Bd IV, Berlin (in German).

Singhvi AK, Banerjee D, Pande K, Gogte V, Valdiya KS (1994). Luminescence studies on neotectonic events in south-central Kumaun Himalaya - a feasibility study. Quaternary Science Reviews (Quaternary Geochronology) 13: 595-600.

Softa M, Spencer JQG, Sözbilir H, Huot S, Emre T (2021). Luminescence dating of Quaternary marine terraces from the coastal part of Eastern Black Sea and their tectonic implications for the Eastern Pontides, Turkey. Turkish Journal of Earth Sciences 30(3):359-378.

Softa M (2022). Morphometric and kinematic analysis of southern margin of the Küçük Menderes Graben and its tectonic implications in western Anatolia. Arabian Journal of Geosciences15(2): 1-21.

Softa M, Utku M (2022). Paleosismoloji çalışmalarında kolüvyal çökellerdeki su içeriğinin lüminesans tarihlendirmeye etkisinin değerlendirilmesi; Soma-Kırkağaç Fayı'ndan bir örnek. Afyon Kocatepe Üniversitesi Fen Ve Mühendislik Bilimleri Dergisi 22(2): 417-430 (in Turkish).

Softa M, Sozbilir H, Sahiner E, Utku M, Buyuktopcu MF (2022). Using The Luminescence Surface Dating In Paleoseismological Studies: Preliminary Findings From The Manisa Fault. 74th Geological Congress of Turkey with international participation 2022. Abstract Book p. 402.

Sohbati R, Murray AS, Jain M, Buylaert JP, Thomsen KJ (2011). Investigating the resetting of OSL signals in rock surfaces. Geochronometria 38(3): 249-258.

Sohbati R, Murray AS, Chapot MS, Jain M, Pederson J (2012a). Optically stimulated luminescence (OSL) as a chronometer for surface exposure dating. Journal of Geophysical Research: Solid Earth 117(B9).

Sohbati R, Jain M, Murray A (2012b). Surface exposure dating of non-terrestrial bodies using optically stimulated luminescence: A new method. Icarus 221(1): 160-166.

Soysal H, Sipahioğlu S, Kolçak D, Altınok Y (1981). Türkiye ve Çevresinin Tarihsel Deprem Kataloğu (2100 B.C.-1900 A.D.). TÜBİTAK Raporu, No. TBAG-341.

Sözbilir H, İnci U, Erkül F, Sümer Ö (2003). An active intermittent transform zone accommodating N-S Extension in Western Anatolia and its relation to the North Anatolian Fault system, International Workshop on the North Anatolian, East Anatolian, and Dead Sea Fault Systems. In Recent Progress in Tectonics and Paleoseismology, and Field Training Course in Paleoseismology. Poster Session P2/2: Ankara

Sözbilir H, Sümer Ö, Uzel B et al. (2007). Geological features of strikeslip basins located within the İzmir-Balıkesir Transfer Zone, western Anatolia. 11th Workshop of Active Tectonics Research Group Meeting, Abstracts, p. 42 (in Turkish).

Sözbilir H, Sarı B, Uzel B, Sümer Ö, Akkiraz S (2011). Tectonic implications of transtensional supradetachment basin development in an extension-parallel transfer zone: the Kocaçay Basin, Western Anatolia, Turkey. Basin Research 23: 423-448. https://doi.org/10.1111/j.1365-2117.2010.00496.x.

Spencer JQ, Owen LA (2004). Optically stimulated luminescence dating of Late Quaternary glaciogenic sediments in the Upper Hunza valley: validating the timing of glaciation and assessing dating methods. Quaternary Science Reviews 23: 175-191.

Spencer JQG, Hadizadeh J, Gratier J-P, Doan ML (2012). Dating deep? Luminescence studies of fault gouge from the San Andreas Fault zone 2.6 km beneath Earth's surface. Quaternary Geochronology 10: 280-284.

Spencer JQG, Robinson RAJ (2008). Dating intramontane alluvial deposits from NW Argentina using luminescence techniques: problems and potential. Geomorphology 93:144-155.

Stahl T, Quigley MC, McGill A, Bebbington MS (2016). Modeling earthquake moment magnitudes on imbricate reverse faults from palaeoseismic data: Fox peak and forest creek faults, South Island, New Zealand. Bulletin of the Seismological Society of America 106(5): 2345-2363.

Stewart IS, Hancock PL (1988). Normal fault zone evolution and fault scarp degradation in the Aegean region. Basin Research 1(3): 139-153.

Sümer Ö (2015). Evidence for the reactivation of a preexisting zone of weakness and its contributions to the evolution of the Küçük Menderes Graben: a study on the Ephesus Fault, Western Anatolia, Turkey. Geodinamica Acta 27 (2-3): 130-154.

Şahiner E, Polymeris GS, Öztürk MZ, Kadioğlu YK, Meriç N (2021). Component resolved equivalent dose estimation using TL glow curves of travertine samples from Anatolia, Turkey. Geochronometria 48(1): 171-178.

Şengör AMC, Görür N, Şaroğlu F (1985). Strike-slip faulting and related basin formation in zones of tectonic escape: Turkey as a case study. In: Biddle K, Christie-Blick N (editors). Strike-slip Deformation, Basin Formation and Sedimentation. 1st ed. Texas, USA: Society of Economic Paleontologists and Mineralogists, Special Publication.

Şengör AMC (1987). Cross-faults and differential stretching of hanging walls in regions of low-angle normal faulting: examples from western Turkey. Geological Society, London, Special Publications 28(1): 575-589.

Şengocmen Geçkin B, Sözbilir H, Özkaymak Ç, Softa M, Spencer JQG et al. (2022). Evidence of surface rupture associated with historical earthquakes on the Gülbahçe Fault Zone (İzmir, Türkiye) and its application for determination of the surface fault-rupture hazard zone. Natural Hazards: https://doi.org/10.1007/s11069-022-05467-9.

Tatumi S H, Batista LR, Watanabe S, Matsuoka M (1989). Thermoluminescence dating of calcite deposits in a Brazilian cave. Nuclear Instruments and Methods in Physics Research Section A: Accelerators, Spectrometers, Detectors and Associated Equipment 280(2-3): 510-513.

Temiz U (2012). Age of fault reactivation by using U/Th dating method of carbonate precipitates: an example from the active Manisa Fault (West Turkey). Geodinamica acta 25(1-2): 1-11.

Thomas PJ, Reddy DV, Kumar D, Nagabhushanam P, Sukhija BS et al. (2007). Optical dating of liquefaction features to constrain prehistoric earthquakes in Upper Assam, NE India - some preliminary results. Quaternary Geochronology 2: 278-283.

Tikhomirov D, Amiri NM, Ivy-Ochs S, Alfimov V, Vockenhuber C et al. (2019). Fault Scarp Dating Tool-a MATLAB code for fault scarp dating using in-situ chlorine-36 supplemented with datasets of Yavansu and Kalafat faults. Data in brief 26: 104476.

Topal S (2019a). Evaluation of relative tectonic activity along the Priene-Sazlı Fault (Söke Basin, southwest Anatolia): insights from geomorphic indices and drainage analysis. Journal of Mountain Science 16(4):909-923.

Topal S (2019b). Karacasu Fayı'nın (GB Türkiye) göreceli tektonik aktivitesinin jeomorfik indislerle incelenmesi. Gümüşhane Üniversitesi Fen Bilimleri Enstitüsü Dergisi 9(1):37-48 (in Turkish).

Trexler CC, Cowgill E, Spencer JQG, Godoladze T (2020). Rate of active shortening across the southern thrust front of the Greater Caucasus in western Georgia from kinematic modeling of folded river terraces above a listric thrust. Earth and Planetary Science Letters 544: 116362

Tsakalos E, Lin A, Kazantzaki M, Bassiakos Y, Nishiwaki T et al. (2020). Absolute Dating of Past Seismic Events Using the OSL Technique on Fault Gouge Material-A Case Study of the Nojima Fault Zone, SW Japan. Journal of Geophysical Research: Solid Earth 125(8) e2019JB019257.

Tsodoulos IM, Stamoulis K, Caputo R, Koukouvelas I, Chatzipetros A et al. (2016). Middle–Late Holocene earthquake history of the Gyrtoni Fault, Central Greece: Insight from optically stimulated luminescence (OSL) dating and palaeoseismology. Tectonophysics 687: 14-27.

Uzel B, Sözbilir H (2008). A first record of a strike-slip basin in Western Anatolia and its tectonic implication: The Cumaovası Basin. Turkish Journal of Earth Sciences 17: 559-591.

Uzel B, Langereis CG, Kaymakci N, Sözbilir H, Özkaymak Ç et al. (2015). Paleomagnetic evidence for an inverse rotation history of western Anatolia during the exhumation of Menderes core complex. Earth and Planetary Science Letters 414: 108-125.

Vafiadou A, Murray AS, Liritzis I (2007). Optically stimulated luminescence (OSL) dating investigations of rock and underlying soil from three case studies. Journal of Archaeological Science 34(10): 1659-1669.

Wallace RE (1981). Active faults, paleoseismology, and earthquake hazards in the western United States. Earthquake prediction: an international review 4: 209-216.

Weismantel O (1891). Die Erdbeben des vorderen Kleinasiens in geschichtlicher Zeit. PhD, Hoher Philosophischer Fakultat der Universitat Marburg, Frankfurt, Germany (in German).

Wessel P, Smith WHF (2006). The Generic Mapping Tools (GMT) version 4.1.4 Technical Reference & Cookbook, NOAA/ NESDIS.

Wintle AG (1975). Effects of sample preparation on the thermoluminescence characteristics of calcite. Modern Geology 5:165- 167.

Wintle AG (1978). A thermoluminescence dating study of some Quaternary calcite: potential and problems. Canadian Journal of Earth Sciences 15(12): 1977-1986.

Zhang J, Wang L (2020). Thermoluminescence dating of calcite–Alpha effectiveness and measurement protocols. Journal of Luminescence 223:117205.

Zreda M, Noller JS (1998). Ages of prehistoric earthquakes revealed by cosmogenic chlorine-36 in a bedrock fault scarp at Hebgen Lake. Science 282(5391): 1097-1099.